Electrochemical and hydrodynamic characterization of a 3D-printed electrochemical flow-cell

Jesús E. Contreras-Naranjo, Víctor H. Perez-Gonzalez, Marco A. Mata-Gómez, Oscar Aguilar*
Tecnologico de Monterrey, School of Engineering and Sciences. Ave. Eugenio Garza Sada 2501, Monterrey, N.L., México, 64849.
* Correspondence: alex.aguilar@tec.mx; Tel.: +52-81-8358-2000 (ext. 4821)

Introduction

This work propose the electrochemical and hydrodynamic characterization of a novel 3D-printed flow-cell integrated with removable commercial-available screen-printed carbon electrodes. Integration of the flow-cell and electrodes resulted in the proposed 3D-printed electrochemical flow-cell adjustable and customizable to detect any desired biomarker. The 3D-printed flow-cell was fabricated through fused deposition modeling (FDM) and the ESCARGOT (Embedded SCAffold RemovinG Open Technology) protocol. Electrochemical and hydrodynamic characterization comprised an experimental and a computational model study respectively, with the purpose to choose the operational working flow rate and to understand the behavior of the fluid through the device. Experimental study was carried out running cyclic voltammetries of $[Fe(CN)_6]^{4-/3-}$ redox probe at different flow rates (0–1000 µL min^{-1}) and the hydrodynamic computational model was performed using COMSOL Multiphysics 5.3a setting physics for laminar flow and transport of diluted species at the same flow rates. Results indicated that the operational working flow rate was 50 µL min^{-1}, and recirculation and vortices zones are formed at flow rates higher than 200 µL min^{-1}.

Experimental

The methodology consisted of the following steps :

a) **Design and fabrication of the electrochemical flow-cell** using 3D-printing and ESCARGOT protocol [1]. The design of the 3D-printed flow-cell was inspired by the commercially available flow-cell from Dropsens. Design and dimensions of the 3D-printed flow-cell were stablished to operate in batch-injection-analysis (BIA) or flow-injection-analysis (FIA) modes. The height (*H*= 4 mm) of the reaction chamber of the flow-cell was designed to work in BIA system using micropipettes.
b) **Electrochemical characterization of the 3D-printed electrochemical flow-cell** The operational flow rate was determined experimentally through electrochemical hydrodynamic using CV at different flow rates different flow rates from 0 to 1000 µL min^{-1}. Hydrodynamic electrochemistry increases the mass transport of biomolecules in a solution compared to stationary conditions, which is reflected in an enhancement of the electrochemical signal and a lower limit of detection (LOD) of the analytical technique [2].
c) **A hydrodynamic computational model** was run to explain the results from CV characterization. The laminar flow state is given based on Re computed for a flow inlet to be Re < 2000 [3].

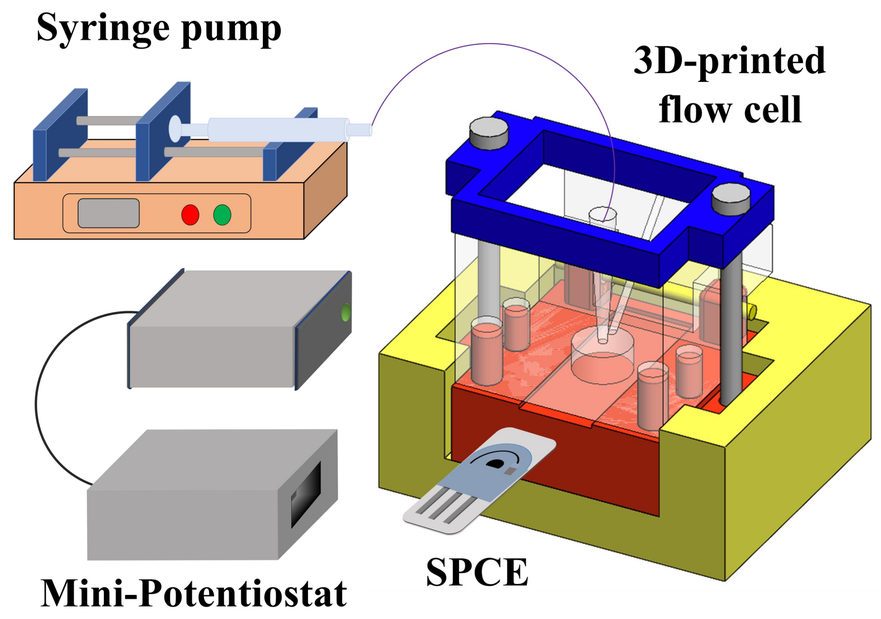

Results

Fabrication and characterization of the 3D-printed electrochemical flow-cell

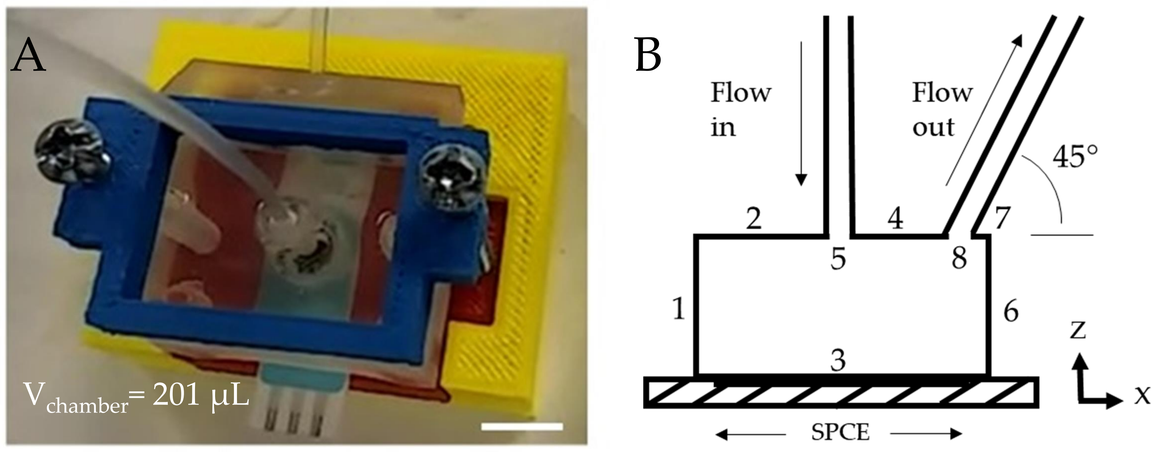

Figure 1. (A) Photograph of a finished prototype for BIA and FIA operation with dimensions in millimeter (50 × 40 × 48; Width × Length × Height). Scale bar represents 1 cm. (B) Inner structure and boundaries of the flow-cell comprising the inlet channel, the outlet channel located at 45° respect to the X axis, and the reaction chamber where is located the commercial SPCE. Boundaries 1 – 4, 6, 7 represent the walls, 5 and 8 the inlet and outlet, respectively.

Table 1. Summary of the boundary conditions used in the numerical simulations of the hydrodynamic behavior of the flow in the 3D-printed electrochemical flow-cell.

Physics	Boundary conditions	Constitutive equation
Laminar flow		
All domains	-	$\rho\,\partial\mathbf{u}/\partial t + \rho(\mathbf{u}\cdot\nabla)\mathbf{u} = \nabla\cdot[-pI + \mu(\nabla\mathbf{u} + (\nabla\mathbf{u})^T)] + \mathbf{F}$
		$\rho\nabla\cdot(\mathbf{u}) = 0$
Boundaries 1-4, 6, 7	No slip	$\mathbf{u} = 0,\ p = 0$
boundary 5	Laminar inflow	$L_{entr}\nabla_t\cdot[-pI + \mu(\nabla_t\mathbf{u} + (\nabla_t\mathbf{u})^T)] = -p_{entr}\mathbf{n}$
boundary 8	Pressure	$[-pI+\mu(\nabla\mathbf{u}+(\nabla\mathbf{u})^T)]\mathbf{n} = -p_0\mathbf{n}$
Transport of diluted species		
All domains	-	$(\partial c_i)/\partial t + \nabla\cdot(-D_i\nabla c_i) + \mathbf{u}\cdot\nabla c_i = R_i$
		$\mathbf{N_i} = -D_i\nabla c_i + \mathbf{u}c_i$
Boundaries 1-4, 6, 7	Insulation	$-\mathbf{n}\cdot\mathbf{N_i} = 0$
boundary 5	inlet	$c_i = c_{0j}$
boundary 8	outlet	$-\mathbf{n}\cdot D_i\nabla c_i = 0$

F stands for the external forces applied to the water, *p* is the fluid pressure, the entrance length (L_{entr}) was 19 mm, *I* is the identity matrix, *T* is the total pressure (Pa), p_{entr} and p_0 represent the pressure at the entrance and the pressure of the system respectively, **n** is the vector normal to a particular boundary, R_i is a production or consumption rate expression (mol m^{-3} s^{-1}), $\mathbf{N_i}$ is the flux vector mol m^{-2} s^{-1} used in boundary conditions and flux computations

Results

Fabrication and characterization of the 3D-printed electrochemical flow-cell

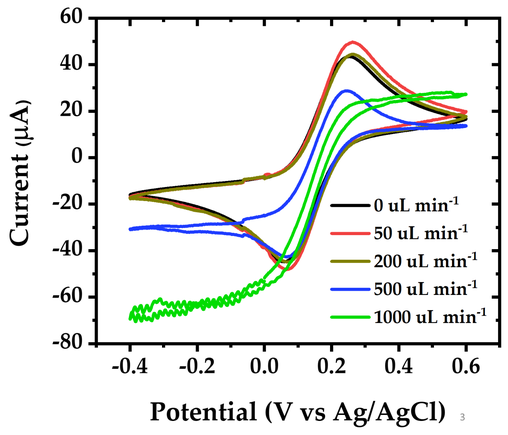

Figure 2. Electrochemical characterization of the flow-cell: CVs of a solution containing 4 mM $[Fe(CN)_6]^{4-/3}$ redox probe in 0.5 M KCl at 50 mV s^{-1} on a non-pretreated SPCE at different flow rates from 0 to 1000 µL min^{-1}.

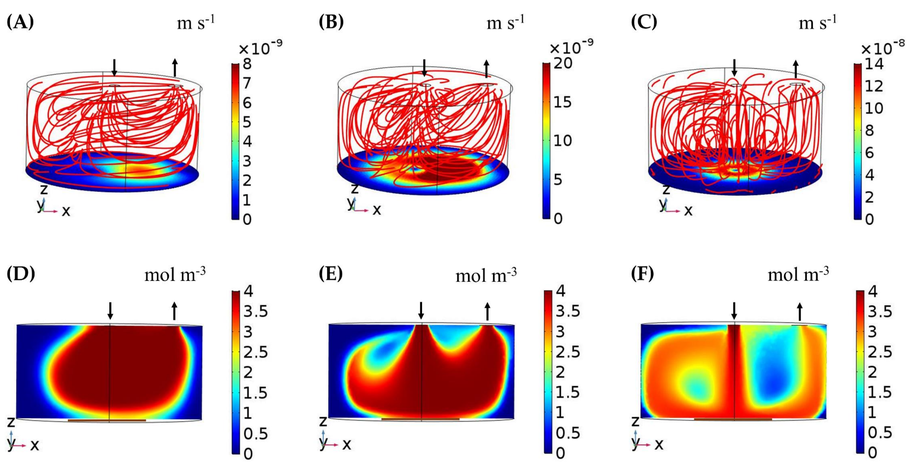

Figure 3. The numerical simulations predict the velocity (A, B, C) (XY plane-top view at Z=0) and concentration (D, E, F) (XZ plane-side view at X=0) profiles of the flow at different flow rates: 50 (A and D), 200 (B and E), and 1000 (C and F) µL min^{-1} for the 3D-printed flow-cell. Streamlines are colored in red in the velocity profile plots, the inlet and outlet of the chamber are presented as down and up arrows, respectively.

Conclusions

- ✓ 3D-printing technology and ESCARGOT protocol, represent alternative techniques in the fabrication of electrochemical sensors and platforms.
- ✓ For our 3D-printed electrochemical platform (*H*= 4 mm, l_{wall} ~ 3 mm), the operational flow rate was 50 µL min^{-1}, based on the current response and the fact that at this flow rate vortices and recirculation zones are not formed. This 3D-printed flow-cell can operate in a flow rate range from 50 up to 200 µL min^{-1}, with an electrochemical performance equal or better compared to only SPCE (stagnant conditions). Also, vortices and recirculation zones are formed within the chamber in a flow rate range of 200 to 1000 µL min^{-1}.

Acknowledgements

Special thanks to Tecnológico de Monterrey, for support this work. Authors would like to thank CONACYT for the doctoral fellowship of Jesús E. Contreras-Naranjo No. 3296.

References

[1] V. Saggiomo, et al., Adv Sci, 2 (2015) 1500125; [2] R. B. Channon, M. B. Joseph, J. V. Macpherson, Interface Magazine 25 (2016) 63–68; [3] Y. Nakayama, R. F. Boucher, *Introduction to fluid mechanics*, Arnold: London, U.K., 1999.